Effect of Partial loss of Spray-on Protection on the Load Capacity of Steel Beams during a Standard Fire

Y. KANG, G. V. HADJISOPHOCLEOUS* AND H. A. KHOO

Department of Civil and Environmental Engineering
Carleton University, Ottawa, Canada

ABSTRACT: Spray-on fire protection is widely used in protecting building members, such as beams, against fire. As this protective coating may be damaged during the service life of the beams, it is essential that the effect of this damage on the fire resistance of a steel beam be understood. A numerical study has been conducted to investigate the reduction in the cross-section moment capacity of protected steel beams exposed to the ISO 834 standard fire due to partial loss of spray-on fire protection. Hot-rolled I-shape steel beams according to CAN/CSA–G40.20/G40.21-98 specifications are used in this study. Results of the study indicate that the reduction of cross-section moment capacity due to the partial loss of protection strongly depends on the area of the protection damage. The reduction of cross-section moment capacity is also affected by several other factors, such as damage shape, damage location, damage penetration, and the weight and depth of the steel section.

KEY WORDS: fire resistance, steel beams, spray-on fire protection, protection loss, cross-section moment capacity.

INTRODUCTION

IT IS KNOWN that the strength and stiffness of steel decrease significantly at elevated temperatures. Owing to the high thermal conductivity of steel, the temperature of unprotected steel members increases rapidly when exposed to fire. As a result, unprotected steel structures do not have desirable resistance against fire. For this reason, spray-on insulation coatings are frequently used to improve the fire resistance of steel members.

*Author to whom correspondence should be addressed. E-mail: george_hadjisophocleous@carleton.ca

1042-3915/08/01 0005–23 $10.00/0 DOI: 10.1177/1042391506074089

SAGE Publications, Los Angeles, London, New Delhi and Singapore

Spray-on fire protection materials have thermal properties that reduce heat transfer from the flames to the steel, and hence lower the rate of steel temperature increase. However, spray-on materials are often very soft, and the protective coatings can be easily damaged during service, resulting in a possible reduction of the fire resistance of the steel member that is being protected.

A few numerical studies have been carried out to investigate the effect of loss of spray-on protection on the fire resistance of steel members. Tomecek and Milke [1] carried out a two-dimensional finite element study to investigate the reduction in fire resistance of steel columns caused by partial loss of spray-on fire protection. Ryder et al. [2] conducted another investigation on steel columns with loss of spray-on fire protection using three-dimensional finite element analyses. However, these articles only looked at local steel temperature rise at the damaged region and used a temperature limit as the fire resistance criterion. The effect of partial loss of protection on the actual load-carrying capacity and deflection of steel members in order to obtain a more rational assessment of fire resistance has not yet been investigated. This article only focuses on the reduction in the load-carrying capacity of steel beams during the ISO 834 standard fire exposure.

METHODOLOGY

The bending moment capacity of protected simply supported steel beams with partial loss of fire protection is investigated using numerical methods. When a protected steel member with partial fire protection loss is subjected to fire exposure, its cross-section within and in the vicinity of the damage area may experience a significant reduction in moment capacity due to the increase of steel temperature. To determine the effect of fire protection loss on the reduction of moment capacity, an uncoupled two-stage numerical analysis, consisting of a heat transfer analysis followed by a structural analysis, is carried out. Each beam investigated is exposed to the ISO 834 standard fire curve.

Steel beams used in the study are CAN/CSA-G40.20/G40.21-98 Grade 350W standard hot-rolled I-shape steel beams listed in CISC [3]. Four I-shape sections, W410 $\times$ 74 (W16 $\times$ 50), W410 $\times$ 60 (W16 $\times$ 40), W310 $\times$ 60 (W12 $\times$ 40), and W310 $\times$ 39 (W12 $\times$ 26) are considered. The imperial designations for these sections are shown in parentheses. Spray-on mineral fiber applied uniformly along the perimeter of the beam cross-section is assumed as the fire protection. Two protection thicknesses, which represent 1- and 2-hour fire resistance ratings for a fully protected steel member,

are considered. The thickness of the protection is estimated using a simple equation from Lie [4], given by

$$d_i = \frac{25.4R}{(1.03W/D + 42)}, \tag{1}$$

where d_i (mm) is the protection thickness, R (min) is fire resistance, W (kg/m) is the weight of the steel section per unit length, and D (mm) is the heated perimeter. It is noted that Equation (1) was originally developed to estimate the thickness of spray-on protection needed for a given fire resistance rating of a steel column subject to the ASTM E119 standard fire exposure. It is adopted in this study because the beams, similar to columns, are assumed to be exposed to fire on four sides in a worst case scenario, and the time–temperature curve of the ISO 834 standard fire is very similar to that of the ASTM E119 standard fire, especially in the first 2 hours. Typically, beams are exposed on only three sides. However, the cross-section moment capacity of an I-shape beam is dependent mainly on the strength of the weaker of the two flanges. Since fire exposure on four or three sides would not produce significantly different temperature distribution at the bottom flange, it is expected that the calculated cross-section moment capacity of the beam with fire exposure on four sides is not overly conservative, when compared to that of a beam exposed on three sides.

Thermal Properties

To predict the load-carrying capacity and deflections, the thermal and mechanical properties of materials are required. The thermal properties involved are density, thermal conductivity, specific heat, and moisture content (for the fire protective material only). The thermal properties of the protective material typically vary with temperature. However, due to lack of reliable data on the temperature-dependence of properties, the constant thermal properties for a spray-on material from ECCS [5], as presented in Table 1, are adopted. In addition, the evaporation of moisture in the

Table 1. Thermal properties of spray-on mineral fiber material, from [5].

Density (kg/m^3)	Thermal conductivity (W/m K)	Specific heat (J/kg K)	Equilibrium moisture content (%)
300	0.12	1200	1

protective material is considered in the analysis, but not the moisture movement. For the steel section, the temperature-dependent specific heat and thermal conductivity of steel at elevated temperatures that are recommended by EC3 [6] are used. Since the volume change of steel at high temperature is small, the density of steel is considered to remain constant with temperature.

EC3 also provides a comprehensive material model for hot-rolled structural steels at elevated temperatures, and is used in the structural analysis. Outinen et al. [7] carried out a series of tests to study the mechanical properties of structural steels at elevated temperatures and compared the test results with that from the EC3 model. Comparisons of the yield strength and the modulus of elasticity between the EC3 model and test results for hot-rolled S355 structural steel are shown in Figures 1 and 2. It can be seen that there is a good agreement between the EC3 model and test results. The protective material is considered to have no strength contribution to the beams.

Heat Transfer Analysis

A heat transfer analysis is carried out to predict the temperature distribution of steel beams in the ISO 834 standard fire exposure. There are two heat transfer processes involved in modeling the standard fire resistance test. One is heat transfer within the specimen, and the other one is the heat exchange at the specimen boundary. In this study, heat transfer within the specimen is through transient heat conduction in a solid body,

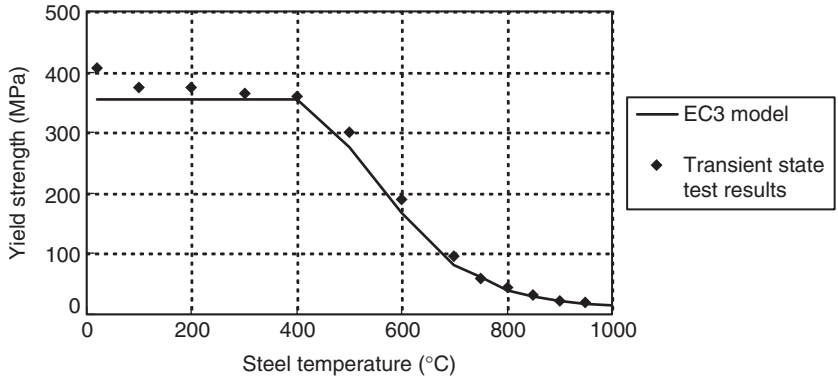

Figure 1. *Yield strength of structural steel S355 at elevated temperatures (adopted from Outinen et al. [7]).*

and heat exchange at the specimen boundary is by convection and radiation. The heat flux acting on the exposed surface, q'' (W/m^2), is given by

$$q'' = h_c(T_f - T_s) + \Phi\varepsilon_{res}\sigma(T_f^4 - T_s^4) \quad \text{with} \tag{2}$$

$$\varepsilon_{res} = \frac{\varepsilon_f\varepsilon_s}{\varepsilon_f + \varepsilon_s - \varepsilon_f\varepsilon_s}, \tag{3}$$

where h_c (W/m^2 K) is the convection coefficient, taken as 25 W/m^2 K for the ISO standard fire (EC1 [8]), T_f(K) is the fire temperature, T_s(K) is the surface temperature, Φ is the view factor, conservatively taken as 1.0, σ is the Stefan–Boltzmann constant, ε_{res} is the resultant emissivity, ε_f is the flame emissivity, taken as 0.8 [9], and ε_s is the surface emissivity, taken as 0.625 for the steel surface [9] and 0.9 for the fire protection surface [2].

The heat transfer analysis was implemented using the finite element program ABAQUS [10]. Two- and three-dimensional finite element heat transfer models were developed to simulate the heat transfer process within the specimen. Two-dimensional finite element models were developed to model the cross-section of fully protected and unprotected steel beams, and three-dimensional models were developed to model the protected steel beams with partial protection loss. Solid bi-linear and tri-linear heat transfer elements DC2D4 and DC3D8 were employed for two- and three-dimensional models, respectively. Thermal properties of steel and the protective material were applied accordingly to elements representing the steel section and the fire protection. The beam with the fire protection loss was assumed to have the plane of symmetry passing through the midspan of the beam. Thus, for a three-dimensional model, only half of the beam

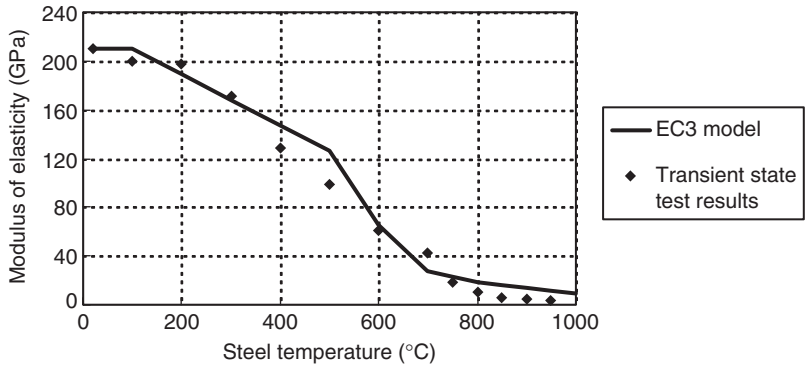

Figure 2. *Modulus of elasticity of structural steel at elevated temperatures (adopted from Outinen et al. [7]).*

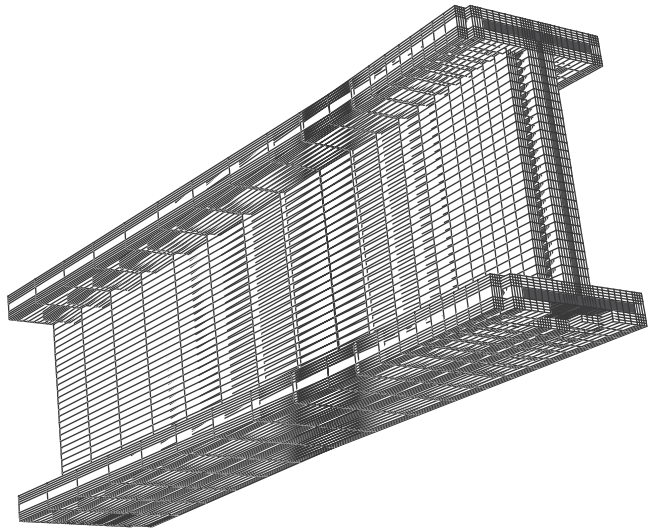

Figure 3. *Finite element heat transfer model of a beam with protection loss on the bottom flange.*

was modeled. Figure 3 shows a three-dimensional model of a protected steel beam with partial protection loss on the bottom flange. It can be seen that the loss of fire protection was modeled by removing elements at the designed damage area. Mesh study was carried out to determine the mesh of the models. The transverse mesh and longitudinal mesh of the models are shown in Figures 4 and 5.

A standard fire resistance test was simulated by conducting a transient heat transfer analysis on a finite element model. Heat flux on the exposed surface was calculated based on the ISO 834 standard fire curve and the boundary condition described by Equations (2) and (3). A user subroutine written in FORTRAN code was developed and used in the analysis to apply the heat flux for the heating process. The temperature profile of a steel beam during heating was obtained through the heat transfer analysis.

Since there was no experimental work involved in this study, test data for model validation were obtained from existing published literature, namely, the data from Ryder et al. [2]. The test from [2] measured the average steel temperature of a W250 $\times$ 73 (W10 $\times$ 49 in imperial designation) steel column covered with 19 mm of spray-on protection in the ASTM E119 standard fire exposure. Two numerical heat transfer analyses were carried out to simulate the fire test from [2], respectively based on the ASTM E119 standard fire

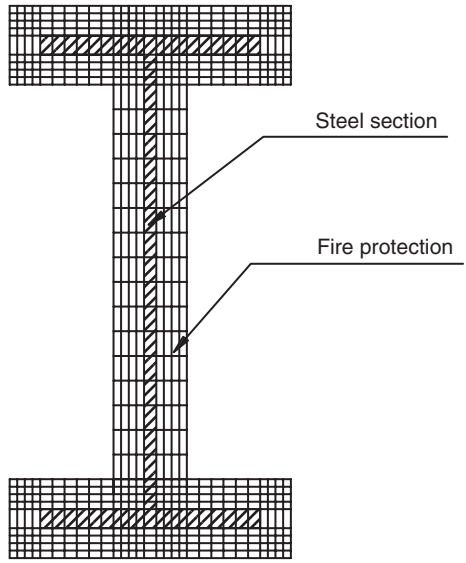

Figure 4. *Transverse mesh.*

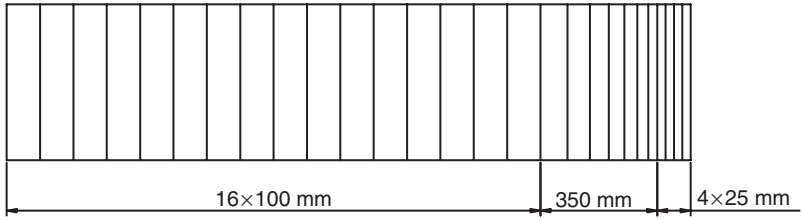

Figure 5. *Longitudinal mesh.*

and the ISO 834 standard fire using the temperature-dependent protective material thermal properties from Ryder et al. [2] and the steel thermal properties from EC3 [6]. The measured average steel temperature and the results of the heat transfer analyses are compared in Figure 6. It can be seen that the predicted steel temperatures based on these two standard fire curves are almost equal, and both match the test result very well.

Another group of test data were obtained from Ding et al. [11]. An H-400 $\times$ 200 $\times$ 8 $\times$ 13 beam protected with 11.3 mm of mineral wool was tested in the Japanese JIS A 1994 standard fire. In the test, the beam was exposed to fire on three sides, leaving the top unexposed and covered with concrete panels. As the author only provided the thermal conductivity

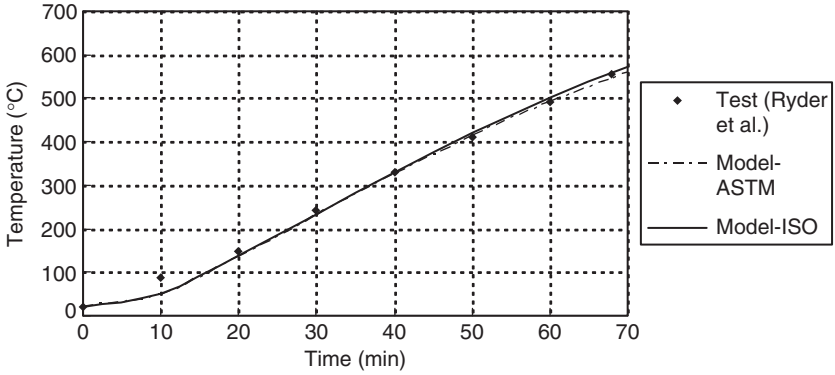

Figure 6. *Average temperature of a W10 × 49 steel column with 19 mm of protection.*

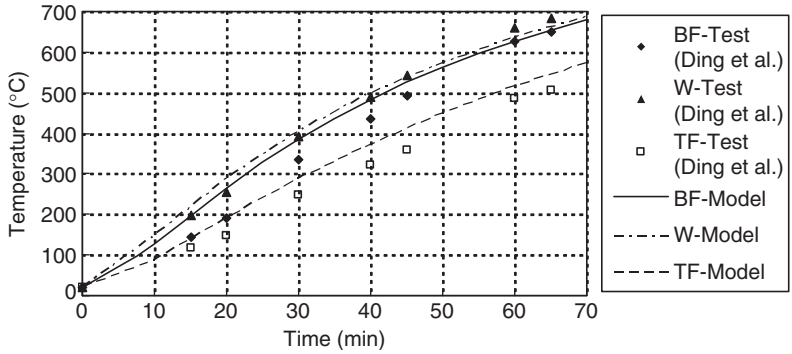

Figure 7. *Temperatures of the bottom flange (BF), top flange (TF), and web (W) for an H-400 × 200 × 8 × 13 steel beam with 11.3 mm of protection.*

of the protective material, 0.13 W/(mK), the other thermal properties of the protective material were taken from Table 1, and the thermal properties of steel were taken from EC3. A heat transfer analysis based on the ISO 834 standard fire curve was conducted to simulate this fire resistance test since the time–temperature curve of the standard fires are quite similar for the time period of the test. The predicted temperature rise of the bottom flange, the top flange, and the web are compared with the test results in Figure 7. It can be seen that the predicted web temperature rise matches the test result very well. The top flange temperature rise is overpredicted during the entire heating period. The bottom flange temperature rise is initially overpredicted, but it becomes very close to the test result after 50 minutes. The discrepancy that appears in Figure 7 may be attributed to two reasons. One reason is

that a constant thermal conductivity of the protective material was used in the analysis. In fact, the thermal conductivity of the protective material increases with temperature. The other reason is that in the numerical analysis, the unexposed surface of the beam was assumed to be completely insulated. In fact, during the fire test, the concrete panels covering the beam act as heat sinks absorbing heat from the beam, causing continuous heat loss from the outer surfaces of these panels. Owing to these reasons, even though there is a discrepancy between predicted and experimental temperatures, it can be concluded that the numerical heat transfer model is valid. It is also known that the heat transfer model is conservatively safe.

Structural Analysis

A structural analysis was carried out to calculate the cross-section moment capacity of steel beams having a non-uniform temperature distribution obtained from the preceding thermal analysis. Formulas for the structural analysis were developed based on classical pure bending theory. In pure bending, the plane section initially perpendicular to the neutral axis of the beam is assumed to remain plane and perpendicular to the neutral axis. For a cross-section with a non-uniform temperature distribution, the moment capacity M_{f} can be calculated with

$$M_{\mathrm{f}} = \sum_{i=1}^{n} \sigma_i A_i y_i, \tag{4}$$

where n is the number of elements in the cross-section, A_i is the area of element i, y_i is the distance from the neutral axis to the centroid of the element I, and σ_i is the average stress of element i. For a steel beam cross-section with no residual stress and with an increasing curvature, the fiber furthest from the neutral axis yields first, and the yield moment $M_{\mathrm{y,f}}$ is given by

$$M_{\mathrm{y,f}} = \sum_{i=1}^{n} \varepsilon_{\mathrm{y},T,0} k_{E,T,i} \frac{E A_i y_i^2}{Y_0}, \tag{5}$$

where $\varepsilon_{\mathrm{y},T,0}$ is the yield strain of the furthest fiber, Y_0 is the distance between the yielded fiber and the neutral axis, and $k_{\mathrm{E},T,i}$ is the reduction factor of elastic modulus at steel temperature T_i. If the cross-section is able to undergo large rotation without any local buckling or distortional buckling,

the plastic moment capacity may be reached. Thus, the plastic moment $M_{p,f}$ can be calculated with

$$M_{p,f} = \sum_{i=1}^{n} k_{y,T,i} f_y A_i y_i, \tag{6}$$

where f_y is the yield stress of steel at normal temperature and $k_{y,T,i}$ is the reduction factor of yield stress at steel temperature T_i. Since the study was confined to standard hot-rolled steel beams, it is unlikely that local buckling on the compression elements of these beams will occur before the yield moment is reached. Residual strain, thermal strain, and strain gradient were not considered since they have little effect on the cross-section moment capacity of simply supported hot-rolled steel beams. In steel structure design codes, steel beams are usually categorized into several class designations according to the curvature that can be attained before local bucking occurs. This is dependent on the width-to-thickness ratio of the elements in compression. The width-to-thickness ratio limit using the ratio of the modulus of elasticity to the yield strength determines if the yield moment or plastic moment can be attained before local buckling occurs. The section classification is employed in the structural analysis, with the width-to-thickness ratio limit of a plate based on the reduced elastic modulus and yield strength at elevated temperatures in the form of

$$\frac{b_e}{t} \leq c\sqrt{\frac{E}{f_y}}, \tag{7}$$

where b_e is the effective width of a plate, t is the plate thickness, and c is a constant that varies for calculating the width-to-thickness ratio limit for different class designations of the section. According to the class designation defined in CAN/CSA S16-01, values of the constant c for Grade 350 steel beams are given in Table 2.

A structural analysis was implemented using Visual Basic programs. The geometrical properties of a beam cross-section were generated in one

Table 2. Values of the constant c for Grade 350 steel.

	Constant c		
Section element	**Class 1**	**Class 2**	**Class 3**
Flange	0.32	0.38	0.45
Web	2.46	3.80	4.25

Visual Basic program, with the cross-section divided into small elements using the same mesh as that in the corresponding heat transfer model. The temperature profile of a steel beam cross-section was input to the program at the beginning of a structural analysis. The moment capacity of a cross-section during a designed standard fire exposure was obtained through the structural analysis.

In addition, a few numerical sequentially coupled thermal-stress analyses were carried out to verify the results of the uncoupled heat transfer and structural analysis. A sequentially coupled thermal-stress analysis consists of two finite element analyses: a heat transfer analysis and a sequential stress analysis. These analyses was implemented using the finite element program ABAQUS. Heat transfer models of the beams were developed using the solid heat transfer element DC3D8. A transient heat transfer analysis was conducted on each model in the same way as the uncoupled heat transfer analysis described previously. Nodal temperatures of a model during heating were stored in a result file and imported into the sequential stress analyses.

The structural models were constructed using solid stress/displacement tri-linear incompatible element C3D8I. The mesh of a structural model was identical to that of a corresponding heat transfer model in order to extract the temperature profile from the result of a heat transfer analysis. The beam modeled was simply supported with lateral supports applied along the compression flange in order to prevent lateral torsional buckling. A uniform distributed load was added on the top flange of the beam. The Riks method option in ABAQUS, a modified arc length method according to Riks [12], was used in the analysis to predict the collapse of the beam.

RESULTS AND DISCUSSION

This study mainly considered the cross-section moment capacity reduction at the midspan cross-section of a steel beam, since the protection loss area is assumed to be symmetric about the midspan of a beam. In addition, the effect of protection loss on the cross-section moment capacity reduction along the length of a beam was also investigated. In order to verify the uncoupled heat transfer and structural analysis, the result of the numerical sequentially coupled thermal-stress analysis is also discussed.

Cross-section Moment Capacity of W410 × 74 Beams

The relative cross-section moment capacities for W410 × 74 beams with symmetric bottom flange protection loss are plotted against fire-exposure

time in Figures 8 and 9, respectively for 1- and 2-hour fire resistance ratings. The relative cross-section moment capacity is the ratio of the cross-section moment capacity at elevated temperatures to that at normal temperature. The size of each protection loss in length × width (cm × cm) is provided in the figures, and the symbol L for beams 1BF11 and 2BF11 represents the full length of a beam. It can be clearly seen that the cross-section moment capacity of a beam with partial protection loss decreases faster than that of its fully protected counterpart. This result is due to the high local temperature profile at the midspan cross-section caused by the partial protection loss.

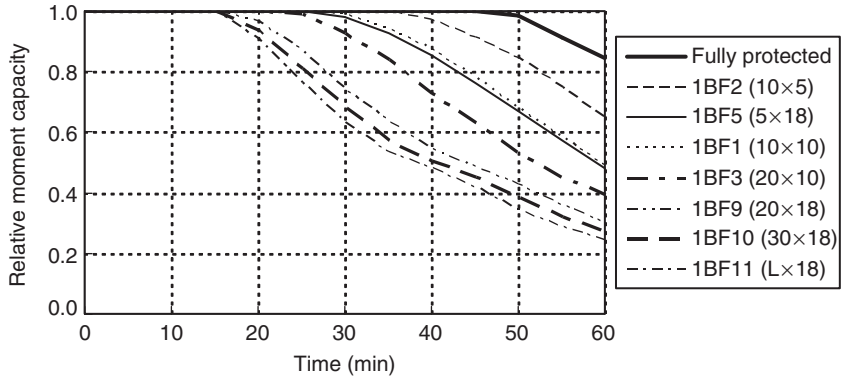

Figure 8. *Relative cross-section moment capacities for 1-hour rating W410 × 74 beams with symmetric bottom flange protection loss.*

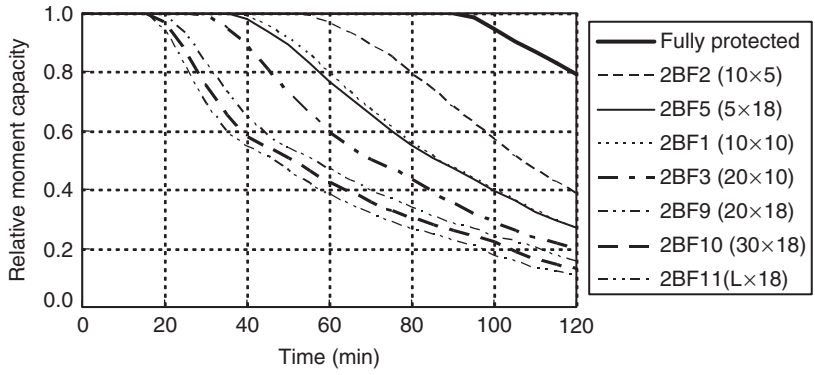

Figure 9. *Relative cross-section moment capacities for 2-hour rating W410 × 74 beams with symmetric bottom flange protection loss.*

Figures 8 and 9 also show that the reduction of cross-section moment capacity strongly depends on the area of protection damage; the larger the damage area, the greater the reduction of the moment capacity. For example, as shown in Figure 8, the cross-section moment capacity of beam 1BF3 (200 cm^2 protection loss) drops to 39% of its initial value after 1 h of standard fire exposure, while that of beam 1BF2 (50 cm^2 protection loss) remains at 65% after the same period of exposure.

The reduction of the cross-section moment capacity is only slightly affected by the shape of the damage. The influence of damage shape can be found by comparing the results between beams 2BF4 and 2BF8 (Figure 10). Both beams 2BF4 and 2BF8 have a protection loss area of 180 cm^2, but the width-to-length ratio of the damage is 1.8 for beam 2BF4 and 0.56 for beam 2BF8. It can be observed that the cross-section moment capacity of beam 2BF4 decreases faster than that of beam 2BF8 during the first 100 minutes, but they decrease at nearly the same rate thereafter. The reason is related to the heat entering from the damage area. At the early stage of fire exposure, the fire temperature rises very fast, and heat enters the steel section through the damage area at a much higher rate than it is conducted away. Therefore, a wider damage shape leads to a faster rate of the local temperature increase in the midspan cross-section due to a wider opening, resulting in a faster reduction rate of moment capacity. According to the time–temperature curve of the standard fire, the fire temperature rises very slowly after a certain time. As a result, the temperature profile of the midspan cross-section becomes more uniform as time progresses. Thus, the influence of damage shape on the moment capacity reduction diminishes. These phenomena indicate that a larger width-to-length ratio of protection damage results in a greater reduction in the moment capacity during early

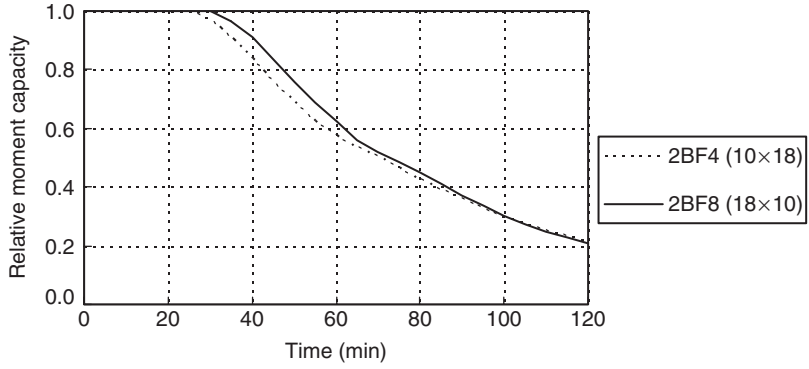

Figure 10. *Relative cross-section moment capacities for W410 × 74 beams 2BF4 and 2BF8.*

stages of standard fire exposure, but this effect becomes smaller for longer fire-exposure time. Overall, the shape of the damage has much less influence than the area of the damage.

Since the fire resistance reduction strongly depends on the area of protection loss, it is possible to characterize the fire resistance reduction using simple equations with respect to the area of protection loss. Hence, the reduction of fire resistance F_r is defined in terms of the ratio of the fire resistance of a beam to its original fire resistance rating, given as:

$$F_r = 1 - \frac{R_f}{R_{f,0}}, \tag{8}$$

where R_f is the time taken for the moment capacity of a beam with a protection loss to drop to the level equal to a fully protected beam at its rated time, and $R_{f,0}$ is the fire resistance rating of the fully protected beam. Two equations are proposed in the following to describe the fire resistance reduction of W410 × 74 beams with the bottom flange protection loss respectively for 1- and 2-hour fire resistance ratings. For 1-hour fire resistance rating, the fire resistance reduction is given by:

$$F_r = 0.635 - \frac{508}{(800 - A_L^{1.4734})}, \tag{9}$$

where A_L is the area of the protection loss. For 2-h fire resistance rating, the fire resistance reduction is given by:

$$F_r = 0.79 - \frac{316}{(400 - A_L^{1.4734})}. \tag{10}$$

Figure 11 shows the fire resistance reductions from Equations (9) and (10) along with the analytical results. For W410 × 74 beams with the bottom flange protection loss at the midspan, the fire resistance reduces rapidly with the damage area when the damage area is less than about 500 cm^2. The rate of reduction reduces as the damage area increases. The fire resistance reduction approaches a limit when the protective coating at the bottom is completely removed. This limit is about 0.635 for 1-hour fire resistance rating W410 × 74 beams and about 0.79 for 2-hour fire resistance rating W410 × 74 beams.

Figure 12 compares the reduction of the cross-section moment capacity for 1-hour fire resistance rating W410 × 74 beams with a 100 mm × 100 mm size protection loss on the bottom flange or on the web. It can be seen that

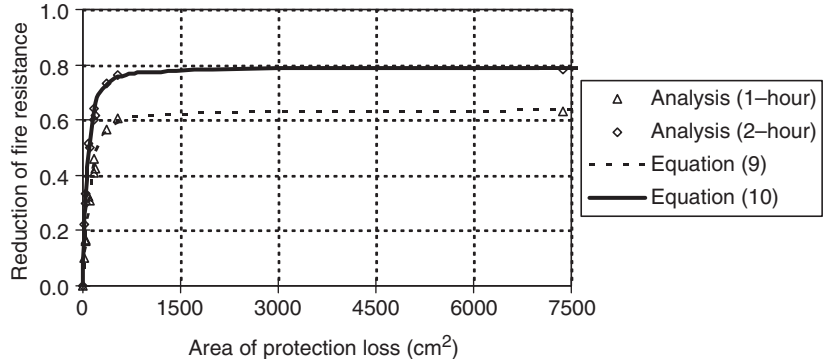

Figure 11. *Fire resistance reductions of 1- and 2-hour rating W410 × 74 beams with the bottom flange protection loss.*

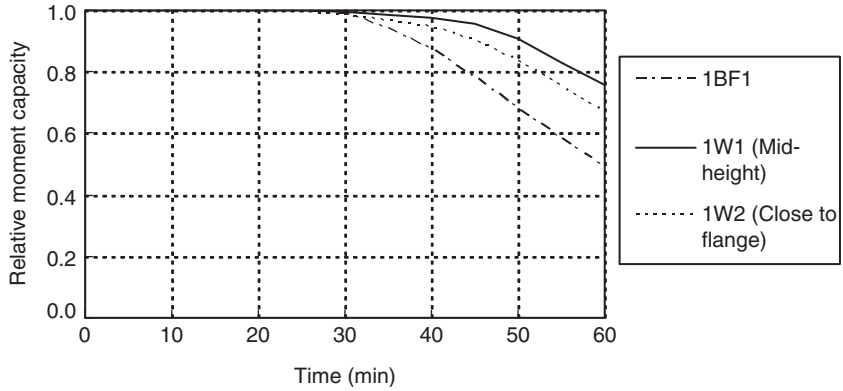

Figure 12. *Relative cross-section moment capacities for 1-hour rating W410 × 74 beams with protection loss on the bottom flange or on the web.*

the flange protection damage has a greater effect on the cross-section moment capacity reduction than the web protection damage. Even among the web protection loss, a protection loss close to the flange (1W2) has a greater effect on the moment capacity reduction than a protection loss at the mid-height of the web (1W1). This is to be expected since the difference in the moment capacity is related to the contribution of different regions of a cross-section to the moment capacity of the cross-section. For an I-shape steel section, the flange has a greater contribution to the cross-section moment capacity than the web. Thus, the weakening of the flange results in a greater reduction in moment capacity than the weakening of the web.

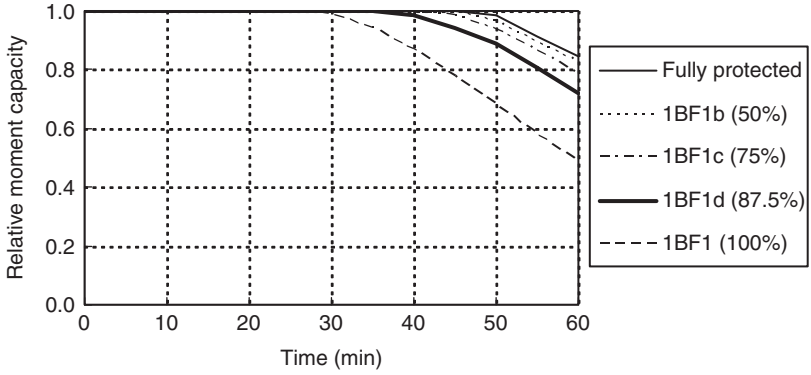

Figure 13. *Relative cross-section moment capacities for 1-h rating W410 × 74 beams with various depths of bottom flange protection loss.*

Similarly, beams with the web protection loss closer to the flange have a greater effect on the moment capacity reduction than those with the protection loss at the mid-height of the web.

The effect of the penetration of the protection damage was also investigated. The investigation was carried out on W410 × 74 beams with a 100 mm × 100 mm size protection loss on the bottom flange. The damage penetration is respectively equal to 100, 87.5, 75, or 50% of the designed protection thickness of a beam. Reductions of the cross-section moment capacity are compared in Figure 13 for 1-hour fire resistance rating beams. It can be seen that a deeper damage penetration results in a larger reduction of the cross-section moment capacity due to a standard fire exposure. However, it can also be observed that the effect of protection loss on the reduction of the cross-section moment capacity is relatively small if the damage does not fully penetrate the protective coating, even when the remaining protection at the damage area is very thin. For example, after 1 hour of standard fire exposure, the relative cross-section moment capacity of beam 1BF1d (with a damage of 87.5% of the protective coating) is only about 15% lower than that of the fully protected beam. The reason may partly be attributed to the large difference between the conductivity of steel and the protective material, and with the conductivity of steel being about 400 times higher. Therefore, heat can be conducted in the steel section at a much higher rate than in the protective material, resulting in a relatively low temperature profile in the steel cross-section even with only a thin layer of protection at the damage area.

To further investigate the moment capacity reduction for beams with a thin remaining protection at the damage area, additional analyses were

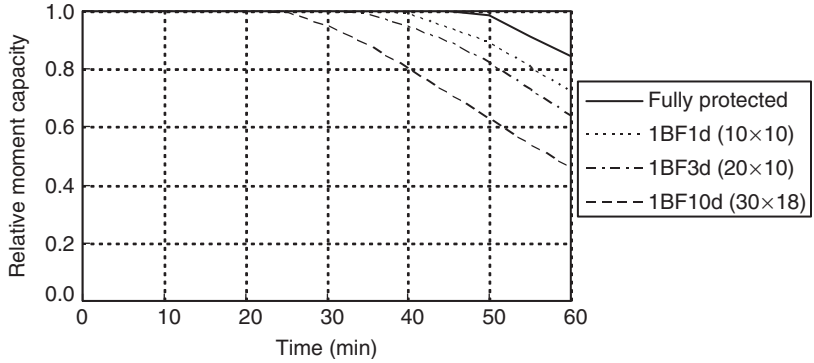

Figure 14. *Relative cross-section moment capacities for 1-hour rating W410 × 74 beams with full protection and with an 87.5% penetrated bottom flange protection loss.*

carried out with W410 × 74 beams for different areas of protection loss. Figure 14 compares the moment capacity reduction for 1-hour rating W410 × 74 beams with full protection and with different protection loss areas of 87.5% damage penetration on the bottom flange. It can be seen that the moment capacity reduction caused by protection loss becomes significant when the protection loss area is large enough, even though there is still a thin remaining protective coating at the damage area. For example, the relative cross-section moment capacity of beam 1BF10d, with a 300 mm × 180 mm size protection loss, is only 46% after 1 hour of standard fire exposure. This value is 39% lower than that of the fully protected beam. On the other hand, it is still significantly better than that with a fully penetrated protection loss where the moment capacity is only 28% after 1 hour, as shown in Figure 8. Thus, the area and the depth of protection loss need to be considered together when assessing the effect of partial loss of fire protection on the fire resistance of steel beams.

Cross-section Moment Capacity of Beams of Different Sections

To compare the effect of protection loss between beams of different steel sections, the cross-section moment capacity reductions of protected steel beams associated with several other steel sections were predicted. Since the cross-section moment capacity reduction is different between fully protected beams of different sections but with identical fire resistance rating, a modified relative moment capacity is used in the comparison to make the effect of the protection loss comparable. The modified relative moment

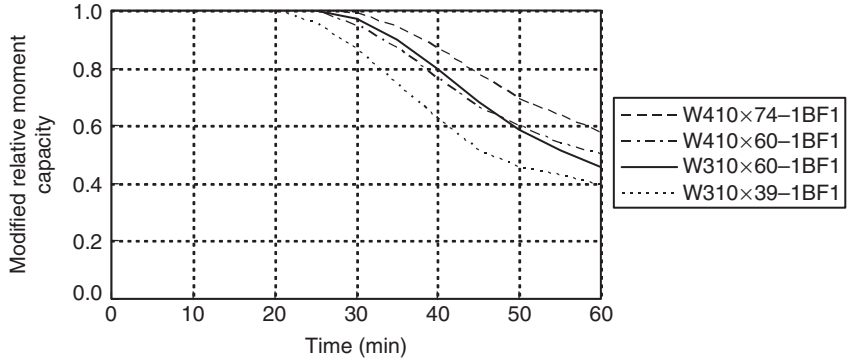

Figure 15. *Modified relative cross-section moment capacities for 1-hour rating W410 × 74, W410 × 60, W310 × 60, and W310 × 39 beams with protection loss on the bottom flange.*

capacity is defined as the ratio of the cross-section moment capacity of a beam with protection loss to that of its fully protected counterpart.

Figure 15 compares cross-section moment capacity reductions between 1-hour rating W410 × 74 and W410 × 60 beams with symmetric protection loss of 100 mm × 100 mm size on the bottom flange. W410 × 74 and W410 × 60 beams have similar depths, but the weight per unit length of a W410 × 74 beam is 26% greater than that of a W410 × 60 beam. It can be seen that the moment capacity reduction of a W410 × 60 beam is greater than that of a W410 × 74 beam. Similar result is found when comparing the moment capacity reduction between a W310 × 39 and a W310 × 60 beam (Figure 15). These results indicate that a beam of a lighter section has a greater reduction of the moment capacity in a fire than that of a heavier section if they both have an identical protection loss. The cause may be attributed to the heat capacity difference between a lighter section and a heavier section. This investigation suggests that Equations (9) and (10) have to be modified for different beam sections.

Figure 16 compares reductions of the cross-section moment capacity between W410 × 60 and W310 × 60 beams with symmetric protection loss of 100 mm × 100 mm size on the bottom flange. W410 × 60 and W310 × 60 beams have similar weights per unit length, but the depth of a W410 × 60 beam is 34% higher that that of a W310 × 60 beam. It can be seen that the moment capacity reduction of the W310 × 60 beam is initially smaller, but it becomes greater than that of W410 × 60 beams in longer fire-exposure time, and the difference of the moment capacity reduction between W410 × 60 and W310 × 60 beams increases with time thereafter. As the flanges of W310 × 60 section are relatively heavier, the W310 × 60 beam has a lower

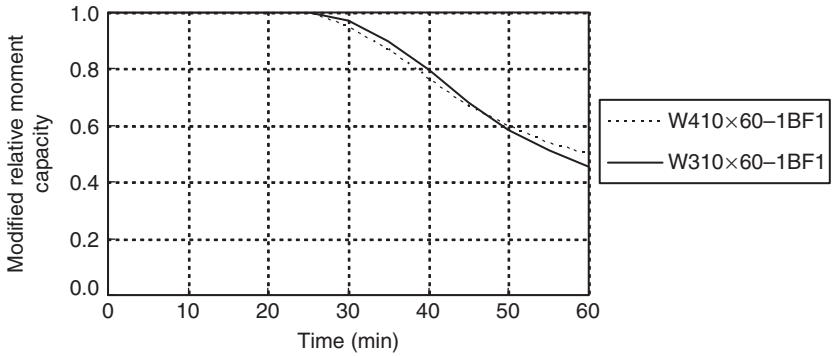

Figure 16. *Modified relative cross-section moment capacities for 1-hour rating W410 × 60 and W310 × 60 beams with protection loss on the bottom flange.*

steel temperature in early fire exposure, resulting in a smaller moment capacity reduction. However, heat entering from the damage area dissipates toward the top flange faster for a section with a lower web. Therefore, compared to the W410 × 60 beam, the W310 × 60 beam has a greater moment capacity reduction in longer fire-exposure time.

Cross-section Moment Capacity along the Length

The influence of protection loss along the length of beams was also investigated. Figures 17 and 18 present modified cross-section moment capacities along the length for 1- and 2-hour fire resistance rating W410 × 74 beams with symmetric bottom flange protection loss after 1 hour of standard fire exposure. It is noted that the origin of the abscissa in Figures 17 and 18 represents the centerline of the damage, and the abscissa value represents the longitudinal distance from the damage center along the length. The results confirm that the largest reduction of the moment capacity occurs on the midspan of a beam or the center of the protection loss. It can be seen that the effect of partial protection loss on the reduction of the moment capacity is very significant at cross-sections within the damage area. However, the effect of protection loss decreases rapidly with distance from the damage area. Taking beam 1BF4 for example, the modified relative cross-section moment capacity is only 0.46 at the edge of the damage area (50 mm from the damage center), and it rises to 0.89 at 200 mm from the damage center. The investigation shows that for 1-hour fire resistance rating W410 × 74 beams, the affected distance is about 400 mm from the edge of the damage area after 1 hour of standard

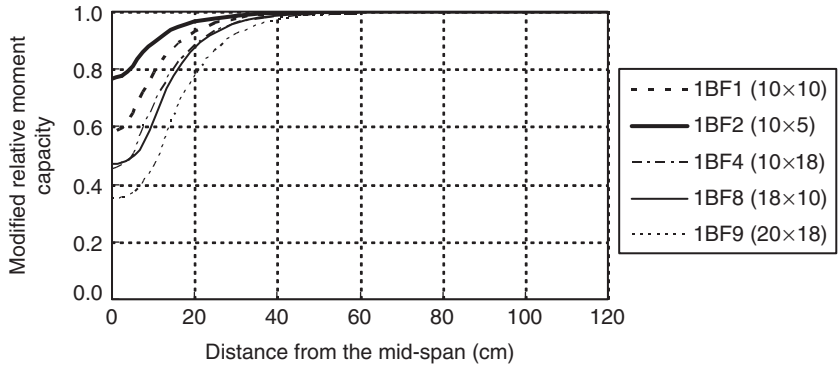

Figure 17. *Modified relative cross-section moment capacities after 1 hour of standard fire exposure for 1-hour rating W410 × 74 beams with symmetric bottom flange protection loss.*

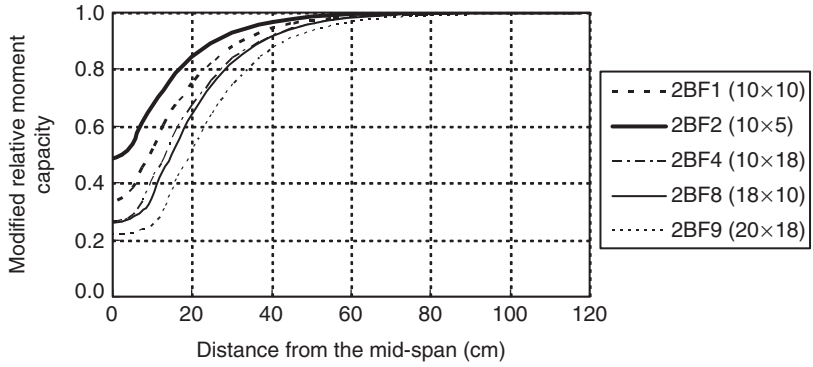

Figure 18. *Modified relative cross-section moment capacities after 1 hour of standard fire exposure for 1-hour rating W410 × 74 beams with symmetric bottom flange protection loss.*

fire exposure. For the 2-hour rating W410 × 74 beams, the affected distance is about 600 mm from the edge of the damage area after 2 hours of standard fire exposure. From the above discussions, it can be concluded that the impact of the partial protection loss becomes less important if the loss does occur close to the critical section of the beam.

Maximum Midspan Moment by Finite Element Modeling

The uncoupled two-stage analysis assumed that the width-to-thickness ratio limit for local buckling as defined in CAN/CSA S16-01 can be applied

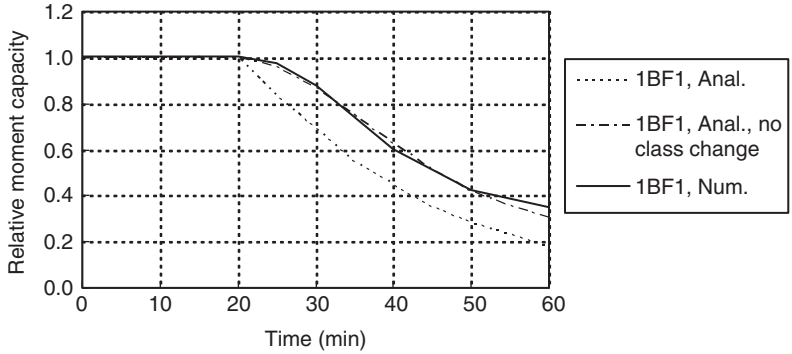

Figure 19. *Relative cross-section moment capacities for 1-hour rating W310 × 39 beams with symmetric bottom flange protection loss.*

to the beam at elevated temperatures. For this reason, numerical sequentially coupled thermal-stress analyses were carried out to verify the validity of this assumption. The relative maximum midspan moment for a 1-hour rating simply supported W310 × 39 beam with a 100 mm × 100 mm size bottom flange protection loss is plotted against fire-exposure time in Figure 19 along with the relative midspan cross-section moment capacity of the beam. The former is the result of finite element structural modeling, and the latter is calculated based on analytical Equations (4)–(7). Figure 16 shows that the predicted numerical maximum moments are consistent with the predicted analytical moment capacities during the whole period of fire exposure if the cross-section class designation change is disregarded. It is noted that from the assumption made for the width-to-thickness limit in the analytical calculation, the cross-section class designation of a W310 × 39 beam will change at about 20 minutes of standard fire exposure. Class 3 section implies that only yield moment before buckling occurs; while Class 2 implies that plastic moment can be attained. Therefore, the cross-section is able to achieve the plastic moments before the class designation changes. But after the class designation change, the compression flange is expected to buckle when the yield stress is reached. However, even though the strain hardening effect of steel was not included in the material model, the finite element analysis predicted the maximum moment capacity equal to the plastic moment. This being that local buckling of the flange involves biaxial stress that enables the load-carrying capacity to be maintained close to its yield strength over a longer range of compressive strain. For this reason, the beam is able to achieve the necessary plastic moment. As a result, the predicted maximum midspan moment in Figure 18 exceeds the yield moment and even reaches the level of the plastic moments. The finite

element analysis shows that the calculated moment capacity using the analytical equations with the assumed width-to-thickness ratio limit for local buckling is conservative. Thus, the analytical procedure can safely be used to calculate the cross-section moment capacity of the beam at elevated temperatures.

CONCLUSIONS

Overall, the study shows that partial loss of spray-on fire protection will cause a reduction of the cross-section moment capacity for protected steel beams under standard fire exposure. The effect of fire protection loss on the cross-section moment capacity reduction strongly depends on the area of protection loss. Moment capacity reduction is also affected by other factors, such as damage shape, damage location, damage penetration, and the weight and depth of the steel section.

With respect to the area of protection loss, the larger the area of protection loss, the greater the reduction in moment capacity. However, the rate of reduction in moment capacity decreases as the area of protection loss increases. For W410 $\times$ 74 beams, the fire resistance reduction approaches a limit of 0.635 after 1 hour and 0.79 after 2 hours of standard fire exposure. The study shows that the shape of protection damage only slightly affects the reduction of the cross-section moment capacity. A larger width-to-length ratio of the damage results in a larger reduction of moment capacity during early stages of standard fire exposure, but this effect diminishes for a longer fire-exposure time. However, the effect of damage shape is much less than that of the area of the damage.

The reduction of the cross-section moment capacity also depends on the location of protection loss. Flange protection loss has a greater effect on moment capacity reduction than web protection loss. For beams with web protection loss, the damage closer to the flange has a greater impact on the moment capacity reduction than that located away from the flange. For beams with a small area of protection loss, the depth of damage penetration has a relatively minor effect on the cross-section moment capacity unless the damage has fully penetrated the protective coating. However, even without the damage being fully penetrated, the cross-section moment reduction becomes significant when the damage area becomes large. On the other hand, the moment reduction is still significantly better than for a beam with the same damage area but with a fully penetrated protection loss.

The weight and depth of the steel section are two factors that affect the cross-section moment capacity reduction. For steel beams with the same section depth but different section weights, the influence of protection loss

on the cross-section moment capacity reduction appears to be greater for the beam with a lighter steel section than the one with a heavier steel section. On the other hand, for steel beams with the same section weight but different section depths, the influence of protection loss is initially greater for the one with a deeper section, but after longer fire-exposure times, the influence of protection loss becomes greater for the beam with a shallower section.

In addition, the effect of partial protection loss on the moment capacity reduction is very significant at cross-sections within the damage area, but this effect decreases rapidly with increase in distance from the damage area. The affected distance is about 400 mm from the edge of the damage area after 1 hour of standard fire exposure for a 1-hour rating W410 × 74 beam, and 600 mm for a 2-hour rating W410 × 74 beam after their rated standard fire exposure.

REFERENCES

1. Tomecek, D.V. and Milke, J.A., "A Study of the Effect of Partial Loss of Protection on the Fire Resistance of Steel Columns," Fire Technology, Vol. 29, No. 1, 1993, pp. 4–21.
2. Ryder, N.L., Wolin, S.D. and Milke, J.A., "An Investigation of the Reduction in Fire Resistance of Steel Columns Caused by Loss of Spray-Applied Fire Protection," Journal of Fire Protection Engineering, Vol. 12, No. 1, 2002, pp. 31–44.
3. CISC, Handbook of Steel Construction, 8th edn, Canadian Institute of Steel Construction, Willowdale, Canada, 2004.
4. Lie, T.T., Structural Fire Protection, American Society of Civil Engineers, New York, USA, 1992.
5. ECCS, Fire Resistance of Steel Structures, ECCS Technical Note No. 89, Technical Committee 3, European Convention for Constructional Steelwork, Brussels, Belgium, 1995.
6. EC3, Eurocode 3: Design of Steel Structures – Part 1-2: General Rules – Structural Fire Design, European Committee for Standardization, Brussels, Belgium, 1995.
7. Outinen, J., Kaitila, O. and Makelainen, P., High-Temperature Testing of Structural Steel and Modeling of Structures at Fire Temperatures, Laboratory of Steel Structures publications: TKK-TER-23, Finland, 2001.
8. EC1, Eurocode 1: Actions on Structures – Part 1-2: General Actions - Actions on Structures Exposed to Fire, European Committee for Standardization, Brussels, Belgium, 2002.
9. Purkiss, J.A., Fire Safety Engineering Design of Structures, Butterworth-Heinemann, Oxford, UK, 1996.
10. ABAQUS Version 6.4.1, ABAQUS/Standard User's Manual, Hibbitt, Karlsson & Sorensen Inc, 2004.
11. Ding, J., Li, G. and Sakumoto, Y., "Parametric Studies on Fire Resistance of Fire-Resistant Steel Members," Journal of Constructional Steel Research, Vol. 60, No. 7, 2004, pp. 1007–1027.
12. Riks, E., "An Incremental Approach to the Solution of Snapping and Buckling Problems," Int. J. Solids Structures, Vol. 15, No. 7, 1979, pp. 529–551.